Available online at www.sciencedirect.com
ScienceDirect
Ceramics International 37 (2011) 2109–2115
CERAMICS INTERNATIONAL
www.elsevier.com/locate/ceramint

Microorganism adhesion inhibited by silver doped Yttria-stabilized zirconia ceramics

Kaijin Xu [a], Yuanyuan Liu [b], Shaomin Liu [c], Aoyang Liu [a], Pengyun Liu [a], Lihong Liu [c,1], Lanjuan Li [a,*]

[a] State Key Laboratory for Diagnosis and Treatment of Infectious Diseases, First Affiliated Hospital, College of Medicine, Zhejiang University, Hangzhou 310003, PR China
[b] Department of Preventive Dentistry, Faculty of Dentistry, National University of Singapore, 5 Lower Kent Ridge Road, Singapore 119074, Singapore
[c] Department of Chemical Engineering, Curtin University, Perth, WA 6845, Australia

Received 10 December 2010; received in revised form 10 January 2011; accepted 27 February 2011
Available online 8 April 2011

Abstract

The aim of this study was to incorporate silver nanoparticles into yttria-stabilized zirconia (YSZ) ceramic for eliminating microorganism adhesion on dental restoration graft. Y_2O_3 (3% mol) partially stabilized ZrO_2 powder with particle size around 80 nm was employed to fabricate tetragonal phase dominated YSZ ceramic block. Silver nanoparticles were efficiently loaded at pH 9.5 by $NaBH_4$ reducing of $AgNO_3$. The biocompatibility of silver incorporated YSZ was evaluated by MTT assay. Antimicrobial activities were quantitatively determined by optical density measurement and qualitatively analysed by scanning electro microscope. Inductively coupled plasma-mass spectrometry (ICP-MS) revealed that YSZ block containing 0.0047 wt% nanosilver, which is safe to mammalian cell, can inhibit the growth of *Escherichia coli*, *Streptococcus mitis* and *Candida albicans*. The pristine YSZ disc had no effect on bacterial growth. This study suggests that silver nanoparticles incorporated into YSZ blocks possess a broad spectrum antimicrobial effect and may help prevent biofilm formation on their surfaces to improve implant survival rate.

Keywords: Sintering; Silver Nanoparticles; Y_2O_3 and ZrO_2; Biomedical applications

1. Introduction

Recently, biomedical zirconia-based ceramics have become commercially available for the restorative and prosthetic community. Yttrium-stabilized zirconia (YSZ) is one of the most commonly used ceramics in dental implants because of its superior mechanical properties and biocompatibility [1,2]. The clinical success and the osteointegration of dental YSZ implants are comparable to or even better than that of titanium, the standard implant material [3]. The growing demand for zirconia in prosthodontics can also be attributed to their esthetics in comparison with traditional metal-based restorations. Environmental friendliness is another advantage of using YSZ ceramics to replace metals and metal alloys (i.e., amalgam) in restorative dentistry [4]. However, despite the high dental implant survival rates (more than 89%), 5-11% of dental implants fail and must be removed [5]. One possible cause of implant failure is associated with biological infection of the peri implant tissues. The adherence of oral microorganisms to YSZ surfaces is recognized as the first step of dental biofilm formation [6,7]. The microbial plaque accumulation could lead to inflammation of the adjacent mucosa and, subsequent bone resorption, increasing the risk of implant failure. Experimental approaches to discouraging initial bacterial attachment to exposed hard material surfaces include hydrophilic anti-bioadhesion coatings [8], antibiotic releasing coatings [9], covalent immobilization of antibiotic on Ti surface [10], and Ag/Zn modification [11,12]. Among the different

* Corresponding author State Key Laboratory for Diagnosis and Treatment of Infectious Diseases, First Affiliated Hospital, College of Medicine, Zhejiang University, Hangzhou 310003, PR China. Tel.: +86 571 87709001; fax: +86 571 87081933.
E-mail addresses: liulihong6@hotmail.com (L. Liu), ljli@zju.edu.cn (L. Li).
[1] Department of Chemical Engineering, Faculty of Science and Engineering, Curtin University of Technology, Australia. Tel: +61 8 82669056; fax: +61 8 92662681.

0272-8842/$36.00
doi:10.1016/j.ceramint.2011.02.023

techniques, the silver incorporation has attracted much attention since several forms of silver have been demonstrated to inhibit the growth of a broad spectrum of microorganisms. Silver nanoparticles are reported effective against *Escherichia coli* [13], and even showed high effectiveness against multiple drug-resistant bacteria, such as methicillin-resistant *S. epidermidis* (MRSE) and methicillin-resistant *S. aureus* (MRSA) [14]. The mechanism of bactericidal effect of silver and silver nanoparticles is still not fully understood. It is generally reported that silver ions binding to thiol groups in enzymes and proteins play an essential role in antimicrobial action. In addition to Ag^+ release, nano silver may be deposited on cell membranes or cell walls to inhibit cell division and disrupt membrane integration [15]. Though silver exhibits a potent antimicrobial activity, it has limited toxicity to mammalian cells. This feature has favoured its use in implant-associated infections treatment [16,17].

Therefore, the aim of the present study was to develop particulate silver-doped zirconia as dental implant materials with the function of eliminating the initial microbial adherence. Three oral microbial species were selected for this preliminary investigation. *Escherichia coli* was chosen as an example of gram-negative bacteria which are responsible for medical device-related infection [18]. *Streptococcus mitis* is a gram-positive bacterium which is commonly found in oral biofilms [19]. *Candida albicans* has been studied with renewed interest, since it is the cause of most oral fungal infections [20] in patients with HIV infection.

2. Materials and methods

2.1. Ceramic implant preparation

ZrO_2 powder partially stabilized by Y_2O_3 (3% mol) with particle size of 60 nm (Shandong, China) was used to prepare zirconia ceramics. The powder was pressed in a stainless steel mould (15 mm in diameter) under a hydraulic pressure of approximately 1.5 x 10^8 Pa. Zirconia ceramic with certain mechanical strength was prepared by sintering the pressed disk in an electric furnace at 1300°C for 5 h under stagnant air, at a heating/cooling rate of 2°C/min. Rectangular ceramic specimens were used for the cytotoxicity and antibacterial assays, respectively. Sterile grafts were cut into rectangular disk under aseptic conditions in a laminar airflow. The weight of each sample was assessed by weighing, because it is easier to control weight than surface area.

Coated zirconia disk were prepared for scanning **electron** microscope by sputtering with gold particles (BAL-TEC MED 020 coating system; Boeckeler Instruments, Tucson, AR) and were examined with a high-vacuum SEM (JSM 6060LV SEM; JEOL Ltd., Tokyo, Japan). The elemental composition of the samples was determined by energy dispersive X-ray spectrometer attached to the above mentioned SEM system. Uncoated YSZ-Ag disk were examined by field emission SEM (Zeiss 1555 VP FESEM, Thornwood, NY) directly.

The X-ray diffraction (XRD) patterns of the YSZ were obtained via Shimadzu X-ray diffractometer using Cu-Kα incident radiation (at a wavelength of λ=1.54056 Å). The generator settings were 40 kV and 30 mA. The diffraction data were collected over a 2θ range of 10-80°, with a scan rate of **0.04°/s**.

2.2. Silver nanoparticle impregnation and silver release

Silver nanoparticles were incorporated into zirconia ceramic by the well-documented chemical reduction technique using $NaBH_4$ (Sigma) as reductant, trisodium citrate dihydrate (VWR International Ltd. England) as a stabilizer and $AgNO_3$ (99.999%, Aldrich Chem. Co.) as the source for the Ag^+ ion. Briefly, 60 mg zirconia disk was immersed in 1 mL of 1 mM $AgNO_3$ for 3 h in a well of 24-well plate, the disk was then transferred to another well and 500 μL of 4 mM trisodium citrate followed by 500 μL of 10 mM sodium borohydride were added to the well under vigorous shaking. A transparent bright brown colour was observed immediately due to the formation of the silver colloid. This colloid was aged for 3 h at 37 °C. ZrO_2 is an amphoteric metal oxide which exhibits both anion- and cation exchange properties depending on the pH and composition of the buffer. In order to increase silver loading efficiency, YSZ-Ag9.5 disk was prepared by immersing YSZ disc in 0.5 mM NaOH (pH = 9.5) solution for 2 h first, then follow the same process for preparing Ag-YSZ5.5 (pH value of DI water is 5.5 in the laboratory).

Inductively coupled plasma-mass spectrometry (ICP-MS) allows the quantitative determination of inorganic species present in implant materials. This technique was used to test silver loading efficiency as well as to monitor the dissolution of Ag^+ leaching from the materials into the culture medium during the assays. Silver release from 60 mg YSZ-Ag prostheses was studied in 10 mL DI water at 37 °C and 100 rpm in a Thermomixer (Fa. Eppendorf, Hamburg, Germany). Rotation was preferred to static state in order to simulate blood flow conditions in the body. A 100 μL aliquot of sample was collected at 2, 6, 10, and 34 h. The resulting solution was diluted 100,000-fold before analysis by ICP-MS. Blank and standard solutions of inorganic silver salts were tested together. The instrument used was PerkinElmer ELAN DYC II analyzer. The Ag detection limit is 1 ppt.

2.3. In vitro cytotoxicity assay, hemocompatibility and antibacterial studies

L929 cells (mouse fibroblast cell line, ATCC, USA) were grown in RPMI (Invitrogen, USA) supplemented with 10% fetal bovine serum, 1% penicillin-streptomycin solution in a humidified atmosphere of 5% CO_2, 95% air at 37 °C. Cells were seeded onto 96-well plates containing YSZ-Ag9.5 graft (15 mg) at a density of 10,000 cells/well. The plates were then returned to the incubator and the cells were allowed to grow as the non-toxic control (medium only). The toxic control experiments were carried out using the complete medium plus 1% Triton X-100 (Sigma). Each condition was tested in eight replicates. 20 μL of MTT (3-[4,5-dimethyl-thiazol-2-yl]-2,5-diphenyltetrazolium bromide, Sigma) solution in 100 μL of fresh medium

was added into each well after 24 hours. The plates were then returned to the incubator and maintained in 5% CO_2, at 37 °C, for further 3 h. The graft, growth medium and excess MTT in each well were then removed. Dimethyl sulfoxide (DMSO, 150 μL) was added to each well to dissolve the internalised purple formazan crystals. An aliquot of 100 μL was taken from each well and transferred to a new 96-well plate. The plates were then assayed at 550 nm and 690 nm using a microplate reader (Power Wave X, Bio-tek Instruments, USA). The absorbance reading of the formazan crystals were taken to be those at 550 nm subtracted by those at 690 nm. The results were expressed as a percentage of the absorbance of the blank. Six samples were tested and the mean values were calculated.

Hemolysis tests were carried out by incubating YSZ-Ag9.5 samples and references in rat blood cells. Fresh red blood cells were washed with PBS for three times. 100 μL of blood cells suspended in PBS (4% in volume) and 15 mg of ceramic graft was added to each well of 96-well plates. Plates were incubated for 1 h at 37 °C. The cell suspensions were taken out and centrifuged at 1000 g for 5 minutes. Aliquots (100 μL) of supernatant were transferred to a new plate, and hemoglobin release was monitored at 576 nm using a microplate reader (Bio-Teck Instruments, Inc). Percentage of hemolysis was calculated using the following formula: Hemolysis (%) = [(O.D.$_{576nm}$ in the nanoparticle solution-O.D.$_{576nm}$ in PBS)/(O.D.$_{576nm}$ in 0.1% Triton X-100 – O.D.$_{576nm}$ in PBS)] × 100.

Strains of *Escherichia coli* (ATCC25922), *Streptococcus mitis* (ATCC6249) and *Candida albicans* (ATCC3153) of clinic interest were obtained from the American type culture collection (Rockville, MD). *S. mitis* were grown in Todd-Hewitt broth (THB). The *E. coli* cultures were maintained in Trypticase soy broth (TSB). Overnight cultures of bacteria were grown in 50 mL centrifuge tube with shaking at 100 rpm at 37 °C. Yeast mould broth was used for overnight cultures of *C. albicans* at 24 °C. All broth was from Difco laboratories, Detroit, MI.

To avoid the potential optical block of YSZ-Ag bulky graft, conventional microdilution method for minimum inhibition concentration test was modified to determine culture turbidity as a qualitative measure of bacterial growth. All 96-well plate and YSZ-Ag substrates were autoclaved for 30 min before the experiments. For determination of antibiotic efficacy at pathologically relevant concentration, 200 μL bacterial suspensions with 1 x 10^3 CFU/mL were incubated with 15 mg samples of YSZ-Ag9.5 for 24 hours at 37 °C. To further investigate the antimicrobial potential of the samples, higher bacterial concentration containing broth (initial optical reading 0.1 at 600 nm) was then added to each 15 mg YSZ-Ag9.5 substrate in a 96-well plate and incubated at 37 °C for certain defined incubation time with shaking. After that, 100 μL broth was transferred to a new well for culture turbidity reading by a microplate reader. All experiments were performed in triplicate with three substrates and the mean values were calculated. For SEM image analysis after 4 h incubation, YSZ substrates were washed twice with PBS before fixing with 3% glutaraldehyde for overnight at 4 °C. After step dehydration with serial ethanol for 10 min each and coated with gold, the surfaces of the substrates were imaged using SEM.

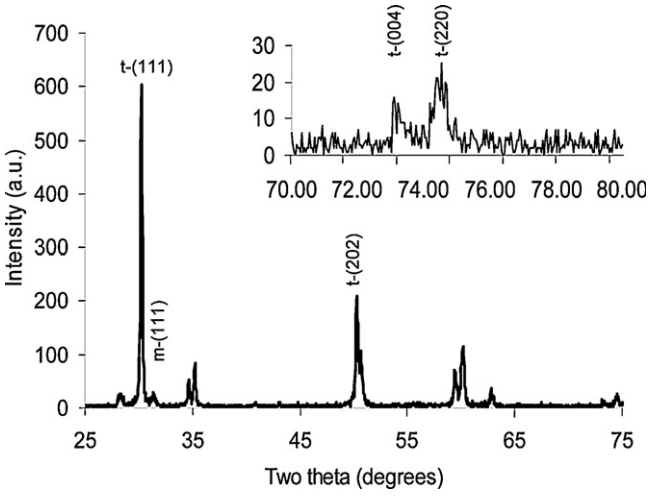

Fig. 1. XRD pattern of prepared YSZ ceramic.

3. Results

3.1. Ceramic characterization

Fig. 1 presents the XRD pattern for the prepared zirconia ceramics. The absence of segregated yttrium compounds indicated homogeneous dispersion of yttrium in YSZ powders. The main peak at 2θ = 30.2° is contributed by (111) reflection of tetragonal YSZ crystallite. The (004) and (220) reflections corresponding to tetragonal phases are also observed in Fig. 1 [21,22]. However, the characteristic reflection of monoclinic phase of (104) appearing at 2θ = 71° is absent in our YSZ dental materials. In addition, no obvious splitting is observed around the 50.2° (2θ) area. If a monoclinic phase is present in substantial amount, the peaks at 49.2° and 50.4° [23] characteristic of monoclinic phase would have appeared. All these results clearly confirm that the 3 mol% yttria-stabilization allowed the tetragonal crystalline phase to predominate, with low amounts of monoclinic phase formed.

The crystallite size was determined by using Scherrer equation D = kλ/β cos θ, where k is the constant related to the shape of the grain (k is about 0.9 for spherical grains), λ the wavelength of X-rays (0.15406 nm), β the full width at half maximum (FWHM) of principal reflection (111) and θ is the Bragg angle. The calculated crystallite size was found to be 45.9 nm. Scanning electron microscopy images (Fig. 2) reveal the near equi-axed shapes of primary particles. The size of these particles lies in the range from ∼100 nm to ∼400 nm. The primary particles appear to densely fuse together and only small voids are observed.

3.2. Silver incorporation and release profile in water

Hydroxide groups with an amphoteric behaviour exist on ZrO_2. The isoelectric point of ZrO_2 is close to 7 [24]. At pH above 7, the ZrO_2 surface is negatively charged and complexation equilibria with silver ions can occur according to:

$$ZrOH \rightarrow ZrO^- + H^+$$

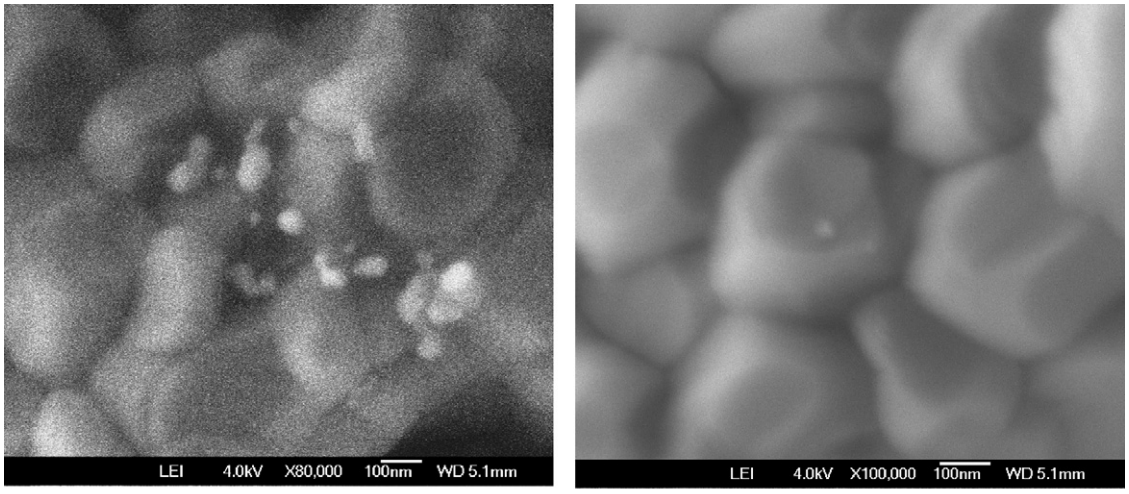

Fig. 2. Silver nanoparticles on the surface of YSZ- Ag 9.5 (a) and YSZ-Ag5.5 (b).

$$ZrO^- + Ag^+ \rightarrow ZrOAg$$

Therefore, we adjusted the pH of the solution to 9.5 in order to promote more Ag + adsorption on the ceramic surface and subsequent higher Ag loading efficiency. The total silver nanoparticle content after washing away unreacted ions was determined by ICP-MS. Compared to reaction at pH 5.5 (in deionized water), the loading efficiency at pH 9.5 was increased from 0.0026 wt% to 0.0047 wt%.

In agreement with ICP-MS results, the SEM micrograph (Fig. 2a) of YSZ-Ag9.5 shows more bright silver nanoparticles on the surface of the ceramic than that of YSZ-Ag5.5 (Fig. 2b). The presence of Ag on the YSZ surface was also confirmed by the EDX analysis. The primary silver nanoparticles are in the range of 10 to 50 nm. Even the slightly aggregated nanoparticles are less than 100 nm, which facilitated a high release of silver ions and consequently high antibacterial activity.

The in vitro Ag release curves are shown in Fig. 3. The release profile gives an indication of how well controlled the release of silver from the ceramic is. This is important, as too high a silver level will damage host cells. It is therefore more effective to have a small amount of silver released in a controlled manner. Both YSZ-Ag9.5 and YSZ-Ag5.5 have low silver content and slow release profiles. Around one third of the silver was released within 34 hours.

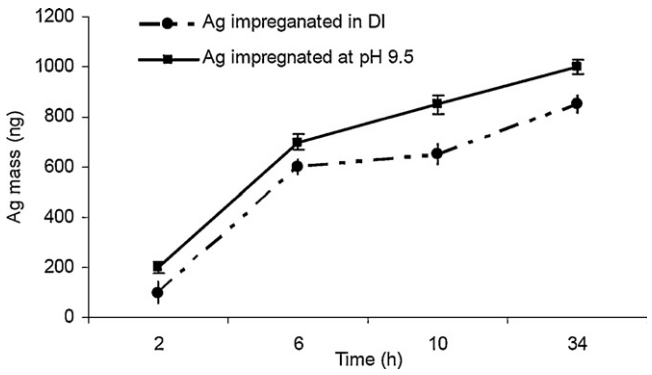

Fig. 3. Silver release profiles in deionized water. Silver loading efficiency is 0.0047% at pH 9.5, and 0.0026% at pH 5.5.

3.3. In vitro cytotoxicity evaluation and antimicrobial test

L929 cells were exposed to YSZ-Ag9.5 for 24 h and cytotoxicity was determined with the MTT assay. Cell viability % of growth medium, YSZ-Ag9.5 and Triton X-100 were 100 ± 1, 98 ± 3 and 1 ± 0.3. There is no apparent evidence of cytotoxicity indicating good biocompatibility in vitro.

Percentage of hemolysis of YSZ-Ag9.5, YSZ and PBS only was 2 ± 0.3, 1 ± 0.4 and 0 ± 0.2, respectively.

As expected, YSZ-Ag9.5 exhibited antibacterial effect toward gram-negative *E. coli*, gram-positive *S. m*itis as well as to the yeast *C. albicans*. However, a control sample (zirconia only) showed no antibacterial activity against any of the three microorganisms (Fig. 4).

Scanning electron microscopy was further used to observe qualitative changes in bacterial adherence density and their morphology change after incubation with YSZ-Ag9.5. In Fig. 5a, after 4 h of incubation, crowds of *E. coli* can be seen on the surface of the control YSZ, and the bacterial cells retained their rod shape. In sharp contrast, only a few flat cells and a large number of cell debris were found on the YSZ-Ag9.5 surface. Clearly, *E. coli* incubated with the YSZ-Ag9.5 for 4 h appeared to undergo the release of their cellular contents, resulting in the very flat cell body (Fig. 5b).

4. Discussion

4.1. Rational design of yttria (3 mol%) stabilized tetragonal ZrO_2

Unalloyed zirconia is monoclinic (m) at room temperature and ambient pressure. The crystallographic structure is tetragonal (t) between 1170 and 2370 °C and cubic (c) above

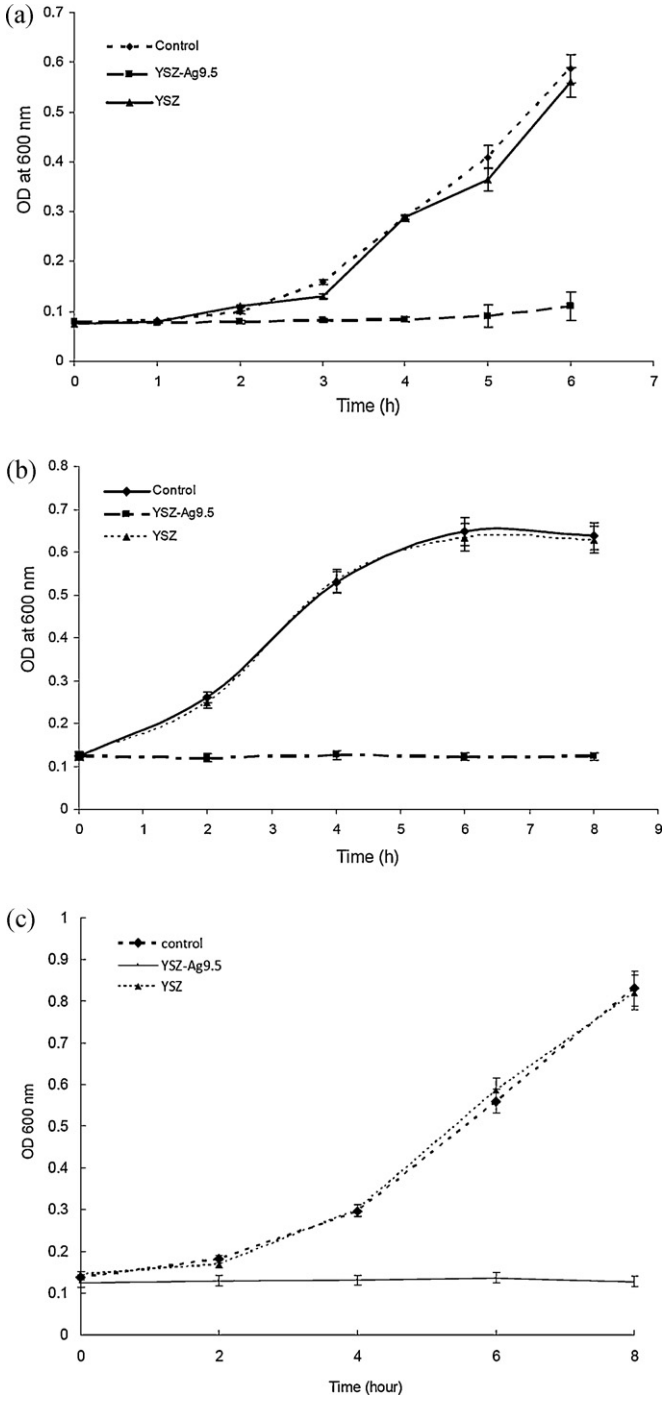

Fig. 4. Silver loaded YSZ inhibited the growth of *E. coli* in TSB medium (4a), *S. mitis* in THB medium (4b) and *C. albicans* in YM medium (4c).

2370 °C and up to the melting point [25]. The lattice transformation from the t phase to the m phase is accompanied by a substantial shape deformation, subsequently leading to microcracking and lower reliability. Therefore, stabilization of pure ZrO_2 has been an important issue to conserve its cubic or tetragonal high-temperature phases upon cooling to room temperature. Our design concept of denture implants is that the employment of 3% Y_2O_3 partially stabilized ZrO_2 (YSZ) powder with initial grain size of 60 nm will lead to the retention of the tetragonal structure at room temperature, thus efficiently arresting crack propagation. The mechanical properties of the YSZ block strongly depend on its particle size, where small grain sizes (<1 μm) are associated with a lower transformation rate because of the large amount of energy required to create new surface area when undergoing the t→m transformation [26]. To obtain insight into the crystalline forms of the block, we used XRD to obtain X-ray diffraction pattern of crushed YSZ powder after a 1300 °C sintering process. In terms of tetragonal/monoclinic zirconia content, Fig. 1 shows that tetragonal zirconia is the predominant phase. If the monoclinic phase is present in substantial amount, the characteristic monoclinic phase peak at 71°, reflection of m-(104) would have appeared. Furthermore, the splitting of (400) at 74° into t-(004) and t-(220) correspond to a tetragonal crystallographic system. These results mean that the destructive phase transformation has been substantially eliminated, thus ensuring the mechanical safety of long-term implants.

4.2. Biocompatibility of the prepared zirconia block

Generally, ZrO_2 ceramic materials are considered to be the most biocompatible of all materials used for dental restoration. There was no evidence of in vivo biological side effects in the zirconia studied in rabbits [27], primates [28], and other mammals [29]. Data on cytotoxicity with zirconia in vitro have been exceptional. Previously, Sjögren [30] et al. have ranked Duceratin T and Duceratin C (all containing Y_2O_3) as non-cytotoxic dental materials after studies by Millipore filter method, the agar overlay method, and MTT assay. By employing Alamar Blue assay and DNA quantitation techniques, Uo [31] studied the reaction of human gingival fibroblasts cultured with a YSZ extract, and no cytotoxicity was detected. However, according to our knowledge, the biocompatibility of silver incorporated YSZ has not been reported. Since the ultimate aim of our research is to confer antibacterial properties in dental implant devices, the concern of cytotoxicity of the fabricated ceramics has to be addressed. In the current study, we incubated the YSZ-Ag9.5 ceramic block with L929 cell line to evaluate the cytotoxicity of both Y_2O_3 and silver. No cytotoxicity of YSZ-Ag9.5 was confirmed by MTT assay. Therefore, our results were consistent with former reports and the impregnated silver dose was considered safe.

4.3. Inhibition growth of bacteria and yeast

The pathogenesis of the periodontal infection is complex and involves multiple interactions between gram-positive and gram-negative organisms within the subgingival biofilm. *Streptococci*, particularly the *S. mitis* group (e.g. *S. oralis, S. mitis*) are considered the primary colonizers to prepare an environment for dental plaque formation. The microbiota associated with failing osteointegrated dental implants show greater proportions of gram-negative anaerobes. Other periopathogenic species such as gram-positive bacteria and C. *albicans* have also been identified around implants. Therefore, in this study, gram-negative *E. coli*, gram-positive *S. mitis* and

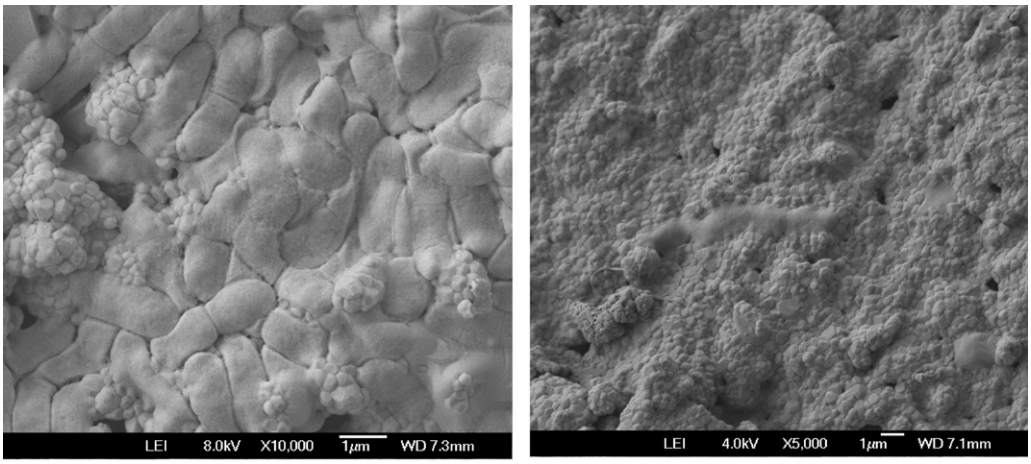

(a) (b)

Fig. 5. External morphology of *E. coli* observed by SEM. (a), incubated with pristine zirconia. (b), incubated with silver loaded YSZ ceramic.

the most isolated *C. albicans* were chosen as model organisms for antimicrobial evaluation.

YSZ-Ag9.5 (at a Ag to YSZ ceramic ratio of 0.0047%) demonstrated a highly effective potency against pathologically relevant *E. coli*, *S. mitis* and *C. alibicans* in the concentration range of 10^2 to 10^4 CFU/mL for 24 h (data not shown). From Fig. 4, it can be seen that with the silver incorporation, bacterial growth in a highly concentrated bacterial suspension of 3 x 10^7 CFU/mL (*E. coli*), 8 x 10^6 CFU/mL (*S. mitis*), and 3 x 10^6 CFU/mL (*C. albicans*) could be inhibited within the testing time.

Representative SEM images of the pristine and silver loaded zirconia ceramic surfaces after 4 h incubation with *E. coli* suspension in TSB broth are shown in Fig. 5. It can be seen that the bacterial cells colonized densely onto the surface of the control YSZ ceramic. In contrast, the extent of bacterial adhesion on the silver loaded ceramic decreased significantly as compared to that on the control. It appears that the effectiveness of silver incorporation on preventing bacterial adhesion is high.

The oral microbial-plaque communities have a complex and diverse ecology. There are more than 500 bacterial taxa have been isolated from oral surfaces. In this study, the coverage of a broad spectrum of pathogens was the crucial factor for antibiotics of choice. Silver nanoparticles were chosen because silver has been known to have strong bactericidal effects since the times of ancient Greece, as well as a broad spectrum of antimicrobial activities [32]. Today, supplied in various forms, such as Ag^+ cation, as metallic silver or as part of composite materials, silver-based compounds are used widely to prevent bacterial colonization on burn wounds, catheters, vascular grafts, and fabrics. Several mechanisms have been proposed to explain the antimicrobial effect of silver. It is generally believed that silver ions interact with the SH groups of enzymes and proteins, which leads to the interference of RNA and DNA replication, and disruption of ion transport processes. In addition, silver nanoparticles may adhere to the surface of the bacterial membrane to disturb permeability and respiration functions of the cell. Contrary to implant materials filled with silver-ion which display fast Ag^+ release, silver nanoparticles can provide a large reservoir of silver ions that can be released gradually and result in long-term antimicrobial activity.

5. Conclusions

Yttria-stabilized zirconia ceramics capable of sustained release of bioactive silver have been prepared. In vitro antimicrobial assays showed that the released silver is effective in eliminating bacterial colonization on the dental prosthesis surface. Additionally, the incorporated silver displays no toxicity and is hemocompatible. The in vitro antimicrobial assays employed in this study are preliminary screens. Currently, we cannot claim that silver nanoparticles at the test concentration exhibited inhibitory activity against the mature biofilm. However, an ounce of prevention equals a pound of cure; once the early bacterial adherence is inhibited, the dental-plaque and peri-implantitis may in turn be prevented. In vivo assessment of activity in a clinically relevant model system will be necessary before proposing the utilization of this technique.

Acknowledgements

This work was funded by State Key Laboratory for Diagnosis and Treatment of Infectious Diseases self-funded research projects (Grant No. 2008ZZ09, 2010ZZ14). The authors gratefully acknowledge the financial support from the Australian Research Council for the project of DP0985578 and Curtin new staff starting up fund.

References

[1] I. Denry, J.K. Robert, State of the art of zirconia for dental applications, Dent. Mater. 24 (2008) 299–307.
[2] L. Rimondini, L. Cerroni, A. Carrassi, P. Torricelli, Bacterial colonization of zirconia ceramic surfaces: an in vitro and in vivo study, Int. J. Oral Maxillofac Implants. 17 (2002) 793–798.
[3] H.J. Wenz, J. Bartsch, S. Wolfart, M. Kern, Osteointegration and clinical success of zirconia dental implants: a systematic review, Int. J Prosthodont. 21 (2008) 27–36.

[4] J.Y. Thompson, B.R. Stoner, J.R. Piascik, Ceramics for restorative dentistry: critical aspects for fracture and fatigue resistance, Mater. Sci. Eng. C. 27 (2007) 565–569.
[5] P.A. Norowski Jr., J.D. Bumgardner, Biomaterial and antibiotic strategies for peri-implantitis, J. Biomed. Mater. Res. B Appl. Biomater. 88B (2009) 530–543.
[6] P.D. Marsh, Microbial ecology of dental plaque and its significance in health and disease, Adv. Dent. Res. 8 (1994) 263–271.
[7] E.M. Lima, H. Koo, A.M. Vacca Smith, P.L. Rosalen, A.A. Del Bel Cury, Adsorption of salivary and serum proteins, and bacterial adherence on titanium and zirconia ceramic surfaces, Clin. Oral. Implants Res. 19 (2008) 780–785.
[8] G Legeay, F. Poncin-Epaillard, C.R. Arciola, New surfaces with hydrophilic/hydrophobic characteristics in relation to (no)bioadhesion, Int. J. Artif. Organs 29 (2006) 453–461.
[9] T. Kalicke, J. Schierholz, U. Schlegel, T.M. Frangen, M. Koller, G. Printzen, D. Seybold, S. Klockner, G. Muhr, S. Arens, Effect on infection resistance of a local antiseptic and antibiotic coating on osteosynthesis implants: An in vitro and in vivo study, J. Orthop. Res. 24 (2006) 1622–1640.
[10] B. Jose, V. Antoci Jr., A.R. Zeiger, E. Wickstrom, N.J. Hickok, Vancomycin covalently bonded to titanium beads kills Staphylococcus aureus, Chem. Biol. 12 (2005) 1041–1048.
[11] A. Ewald, S.K. Gluckermann, R. Thull, U. Gbureck, Antimicrobial titanium/silver PVD coatings on titanium, Biomed. Eng. Online 5 (2006) 22.
[12] P. Petrini, C.R. Arciola, I. Pezzali, S. Bozzini, L. Montanaro, M.C. Tanzi, P. Speziale, L. Visai, Antibacterial activity of zinc modified titanium oxide surface, Int. J. Artif. Organs 29 (2006) 434–442.
[13] I. Sondi, B. Salopek-Sondi, Silver nanoparticles as antimicrobial agent: a case study on E. coli as a model for Gram negative bacteria, J. Colloid Interf. Sci. 275 (2004) 177–182.
[14] V. Alt, T. Bechert, P. Steinrücke, M. Wagener, P. Seidel, E. Dingeldein, E. Domann, R. Schnettler, An in vitro assessment of the antibacterial properties and cytotoxicity of nanoparticulate silver bone cement, Biomaterials 25 (2004) 4383–4391.
[15] S. Shrivastava, T. Bera, A. Roy, G. Singh, P. Ramachandrarao, D. Dash, Characterization of enhanced antibacterial effects of novel silver nanoparticles, Nanotechnology 18 (2007) 225103–225112.
[16] S. Ohashi, S. Saku, K.J. Yamamoto, Antibacterial activity of silver inorganic agent YDA filler, J. Oral Rehabil. 31 (2004) 364–367.
[17] C.N. Lok, C.M. Ho, R. Chen, Q.Y. He, W.Y. Yu, H. Sun, P.K. Tam, J.F. Chiu, C.M. Che, Silver nanoparticles: partial oxidation and antibacterial activities, J Biol. Inorg. Chem. 12 (2007) 527–534.
[18] R.O. Darouiche, Device-associated Infections: a macroproblem that starts with microadherence, Clin. Infect. Dis. 33 (2001) 1567–1572.
[19] L. Sbordone, C. Bortolaia, Oral microbial biofilms and plaque-related diseases: microbial communities and their role in the shift from oral health to disease, Clin. Oral Invest. 7 (2003) 181–188.
[20] D.R. Radfordl, S.J. Challacombe, J.D. Walter, Denture plaque and adherence of Candida albicans to denture-base materials in vivo and in vitro, Crit. Rev. Oral. Biol. Med. 10 (1999) 99–116.
[21] M.P. Rigney, E.F. Funkenbusch, P.W. Carra, Physical and chemical characterization of microporous zirconia, J. Chrom. A. 499 (1990) 291–304.
[22] C. Viazzi, J. Bonino, F. Ansart, A. Barnaḃe, Structural study of metastable tetragonal YSZ powders produced via a sol–gel route, J. Alloys Compd. 452 (2008) 377–383.
[23] Y.B. Khollam, A.S. Deshpande, A.J. Patil, H.S. Potdar, S.B. Deshpande, S.K. Date, Synthesis of yttria stabilized cubic zirconia (YSZ) powders by microwave-hydrothermal route, Mater. Chem. Phys. 71 (2001) 235–241.
[24] G. Dell'Agli, S. Esposito, G. Mascolo, M.C. Mascolo, C. Pagliuca, Films by slurry coating of nanometric YSZ (8 mol% Y2O3) powders synthesized by low-temperature hydrothermal treatment, J. Eur. Ceram. Soc. 25 (2005) 2017–2021.
[25] E.C. Subbarao, Advances in Ceramics, vol. 3, Zirconia-an overview. In: Heuer AH, Hobbs LW, editors. Science and technology of zirconia. The American Ceramic Society, Columbus, OH; 1981, pp 1-24.
[26] A.H. Heuer, N. Claussen, W.M. Kriven, M. Ruhle, Stability of tetragonal ZrO2 particles in ceramic matrices, J Am Ceram Soc. 65 (1982) 642–650.
[27] R.C. Garvie, C. Urbani, D.R. Kennedy, J.C. McNeuer, Biocompatibility of magnesia partially stabilized zirconia (MG, PSZ) ceramics, J. Mater. Sci. 19 (1984) 3224–3228.
[28] J.D. Helmer, T.D. Driskell. Research on bioceramics. Symp. On Use of Ceramics as Surgical Implants. South Carolina (USA), Clemson University, 1969.
[29] C. Piconi, G. Maccauro, Zirconia as a ceramic biomaterial, Biomaterials 20 (1999), 1 25.
[30] G. Sjögren, G. Sletten, J.E. Dahl, Cytotoxicity of dental alloys, metals, and ceramics assessed by Millipore filter, agar overlay, and MTT tests, J. Prosthet Dent. 84 (2000) 229–236.
[31] M Uo, G. Sjören, A. Sundh, F. Watari, M. Bergman, U. Lerner, Cytotoxicity and bonding property of dental ceramics, Dent. Mater. 19 (2003) 487–492.
[32] Q.L. Feng, J. Wu, G.Q. Chen, F.Z. Cui, T.N. Kim, J.O. Kim, A mechanistic study of the antibacterial effect of silver ions on Escherichia coli and Staphylococcus aureus, J. Biomed. Mater. Res. 52 (2000) 662–668.